

Influence of basin-scale and mesoscale physical processes on biological productivity in the Bay of Bengal during the summer monsoon

K.R. Muraleedharan ^a, P. Jasmine ^a, C.T. Achuthankutty ^{a,*}, C. Revichandran ^a,
P.K. Dinesh Kumar ^a, P. Anand ^b, G. Rejomon ^a

^a National Institute of Oceanography, Regional Centre, Dr. Salim Ali Road, P.O. Box 1913, Kochi 682 018, India

^b Naval Physical Oceanographic Laboratory, Thrikkakara, Kochi 682 021, India

Abstract

Physical forcing plays a major role in determining biological processes in the ocean across the full spectrum of spatial and temporal scales. Variability of biological production in the Bay of Bengal (BoB) based on basin-scale and mesoscale physical processes is presented using hydrographic data collected during the peak summer monsoon in July–August, 2003. Three different and spatially varying physical processes were identified in the upper 300 m: (I) anticyclonic warm gyre offshore in the southern Bay; (II) a cyclonic eddy in the northern Bay; and (III) an upwelling region adjacent to the southern coast. In the warm gyre (>28.8 °C), the low salinity (33.5) surface waters contained low concentrations of nutrients. These warm surface waters extended below the euphotic zone, which resulted in an oligotrophic environment with low surface chlorophyll *a* (0.12 mg m^{-3}), low surface primary production ($2.55 \text{ mg C m}^{-3} \text{ day}^{-1}$) and low zooplankton biomass (0.14 ml m^{-3}). In the cyclonic eddy, the elevated isopycnals raised the nutricline upto the surface ($\text{NO}_3\text{-N} > 8.2 \text{ } \mu\text{M}$, $\text{PO}_4\text{-P} > 0.8 \text{ } \mu\text{M}$, $\text{SiO}_4\text{-Si} > 3.5 \text{ } \mu\text{M}$). Despite the system being highly eutrophic, response in the biological activity was low. In the upwelling zone, although the nutrient concentrations were lower compared to the cyclonic eddy, the surface phytoplankton biomass and production were high ($\text{Chl } a - 0.25 \text{ mg m}^{-3}$, $\text{PP} - 9.23 \text{ mg C m}^{-3} \text{ day}^{-1}$), and mesozooplankton biovolume (1.12 ml m^{-3}) was rich. Normally in oligotrophic, open ocean ecosystems, primary production is based on ‘regenerated’ nutrients, but during episodic events like eddies the ‘production’ switches over to ‘new production’. The switching over from ‘regenerated production’ to ‘new production’ in the open ocean (cyclonic eddy) and establishment of a new phytoplankton community will take longer than in the coastal system (upwelling). Despite the functioning of a cyclonic eddy and upwelling being divergent (transporting of nutrients from deeper waters to surface), the utilization of nutrients leading to enhanced biological production and its transfer to upper trophic levels in the upwelling region imply that the energy transfer from primary production to secondary production (mesozooplankton) is more efficient than in the cyclonic eddy of the open ocean. The results suggest that basin-scale and mesoscale processes influence the abundance and spatial heterogeneity of plankton populations across a wide spatial scale in the BoB. The multifaceted effects of these physical processes on primary productivity thus play a prominent role in structuring of zooplankton communities and could consecutively affect the recruitment of pelagic fisheries.

Keywords: Warm gyre; Cyclonic eddy; Upwelling; Mesozooplankton; New production; Regenerated production; Bay of Bengal

* Corresponding author. Tel.: +91 484 2390814; fax: +91 484 2390618.

E-mail address: achu@nio.org (C.T. Achuthankutty).

1. Introduction

Seasonally reversing monsoon winds and associated circulation patterns generate both basin-scale and mesoscale processes that have dominant influences on the biogeochemistry of the Bay of Bengal (BoB). The general hydrography and circulation of BoB have been well studied by Varkey et al. (1996) and Shankar et al. (2002). These studies reported low sea surface salinities, particularly in the northern region of the BoB as a result of the heavy monsoonal precipitation that has an annual average of 2 m (Gill, 1982) and large fresh-water influxes from the Ganges, Brahmaputra and Irawaddy rivers $1.5 \times 10^{12} \text{ m}^3$ (UNESCO, 1988). The excess of precipitation (P) over evaporation (E) during the summer monsoon is a significant source of freshwater to the BoB (Prasad, 1997), which together with the large riverine outflows generates highly stable stratification in the upper layers of the northern BoB. The stratification forms a strong 'barrier layer' to the re-supply of nutrients from deeper waters during the summer monsoon (Lukas and Lindstrom, 1991; Sprintall and Tomczak, 1992; Vinayachandran et al., 2002; Prasannakumar et al., 2002). This barrier persists throughout the late summer and post-monsoon periods, and the associated hydrographic characteristics will have a profound influence on the biological productivity.

The BoB is generally considered to have a lower biological productivity than its western counterpart, the Arabian Sea. Although the rivers may bring nutrients, these are thought to be removed in the deeper waters because of the narrow shelf (Qasim, 1977; Sengupta et al., 1977). The poor solar irradiance during the summer monsoon because of the heavy cloud cover contributes to the low levels of primary productivity.

Most previous biological studies in the BoB focused mainly on the seasonal variation in primary productivity and to some extent on the abundance and composition of mesozooplankton (Panikkar and Rao, 1973; Nair et al., 1981; Achuthankutty et al., 1980; Madhupratap et al., 2003). The transfer of primary production to upper trophic levels and the associated distributional patterns of mesozooplankton have not been studied in the context of basin-scale hydrographic processes.

Mesoscale processes like cyclonic eddies, play a significant role in the re-supply of nutrients to the photic zone, which enhances primary production inside them (Falkowski et al., 1991). Even though the upper layers of the BoB are so stably stratified, eddy pumping is a possible mechanism for transferring nutrients into the euphotic zone and increasing biological production (Gomes et al., 2000; Prasannakumar et al., 2004). Variations in the primary production related to the mesoscale processes and associated changes in the upper trophic levels of the BoB are yet to be elucidated.

During the summer monsoon, southwesterly winds that are prevalent across the east coast of India are favourable for offshore Ekman transport and vertical advection. LaFond (1957), Murty and Varadachari (1968), Shetye et al. (1991) and Rao (2002) have reported upwelling along the coasts of the BoB during summer monsoon. The wind driven vertical advection and mixing has been observed transporting nutrients from within and below the thermocline up into the euphotic zone, replenishing the nutrient concentrations in the upper layers of the BoB during the summer monsoon (Bhavanarayana and La Fond, 1957; Udayavarma Thirupad and Gangadhara Reddy, 1959). Madhu et al. (2002) reported primary production and chlorophyll *a* distribution in the upwelling regions of the southwestern BoB during summer monsoon. The response of mesozooplankton to the coastal upwelling along the west coast of India was studied by Madhupratap et al. (1990). However, similar studies are scarce for the east coast.

Physical processes strongly determine the spatial and temporal structure of biological processes in the ocean. Gyres, eddies and upwelling are highly energetic processes that affect nutrient cycles and biological production, and the distribution and behavior of pelagic organisms. However, very little information exists for the BoB about basin-scale and mesoscale processes or their effects on the composition of marine zooplankton

communities. This information is of fundamental importance for elucidating the distribution of primary production (phytoplankton) and its transfer to pelagic consumers (zooplankton and micronekton) and to higher trophic levels in the food web. This study is an attempt to understand the physical processes and their complex effects on biological production ('regenerated production', 'new production' and 'enhanced new production'), that play prominent roles in structuring of zooplankton communities and consequently in the recruitment of pelagic fisheries.

2. Data and methodology

Hydrographic and biological measurements were carried out in the Bay of Bengal during 9 July–6 August 2003 onboard FORV *Sagar Sampada* as a part of the Marine Research on Living Resources (MR-LR) programme (Cruise SS 215). Stations were distributed along four zonal transects from 11°30' N to 17°30' N (Fig. 1). The transects were set 2° of latitude apart, while the stations were separated by 1° of longitude. An SBE Seabird 911 plus CTD was used to obtain temperature and salinity profiles from each station. Data from Array for Real-time Geostrophic Oceanography (ARGO) buoys were used for high spatial resolution hydrographic data. Salinity values from CTD and ARGO were calibrated against an Autosol (Guildline 8400) onboard. Surface meteorological parameters were acquired at all stations and along the ship's track by the shipborne, automated weather station. The mixed layer depth (MLD) was determined as the depth where the density difference from the surface was 0.2 kg m^{-3} (Shetye et al., 1996). The dynamic topography at 10 m was computed with reference to 1000 m level. Potential temperature – salinity profiles (Fig. 2) from within the three distinct features observed during the study showed that the variations below 300 m were insignificant.

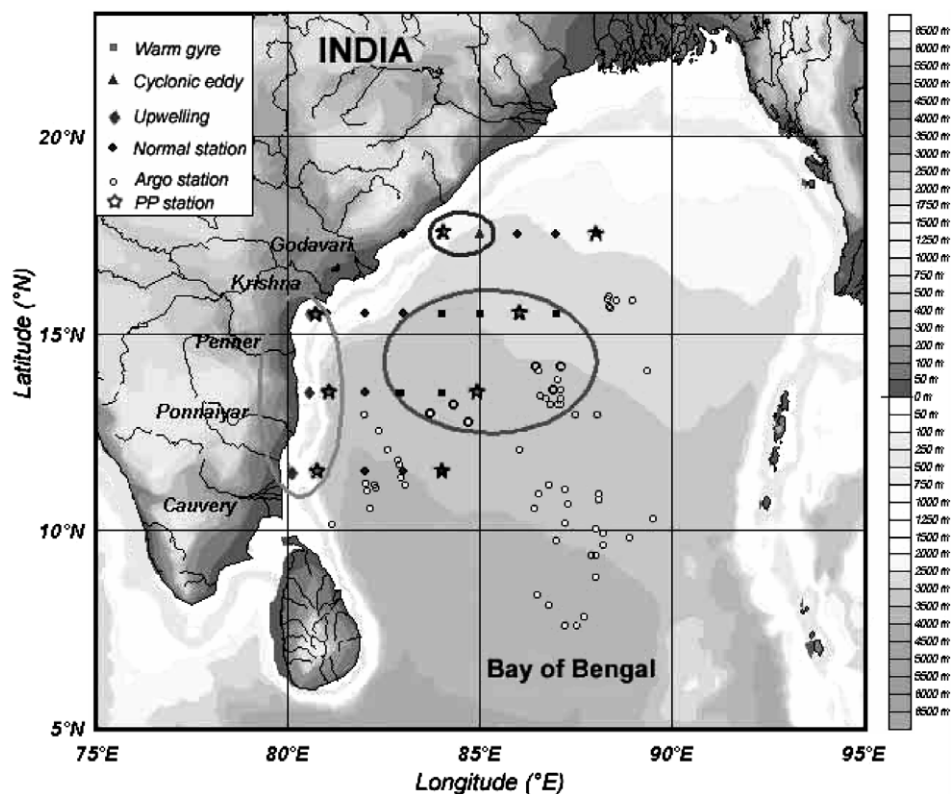


Fig. 1. Bay of Bengal; North-eastern Indian Ocean, showing hydrographic and biological stations on the bathymetric chart. Stations in the circles showed characteristics of warm gyre, cyclonic eddy and upwelling during the summer monsoon (July–August) of 2003.

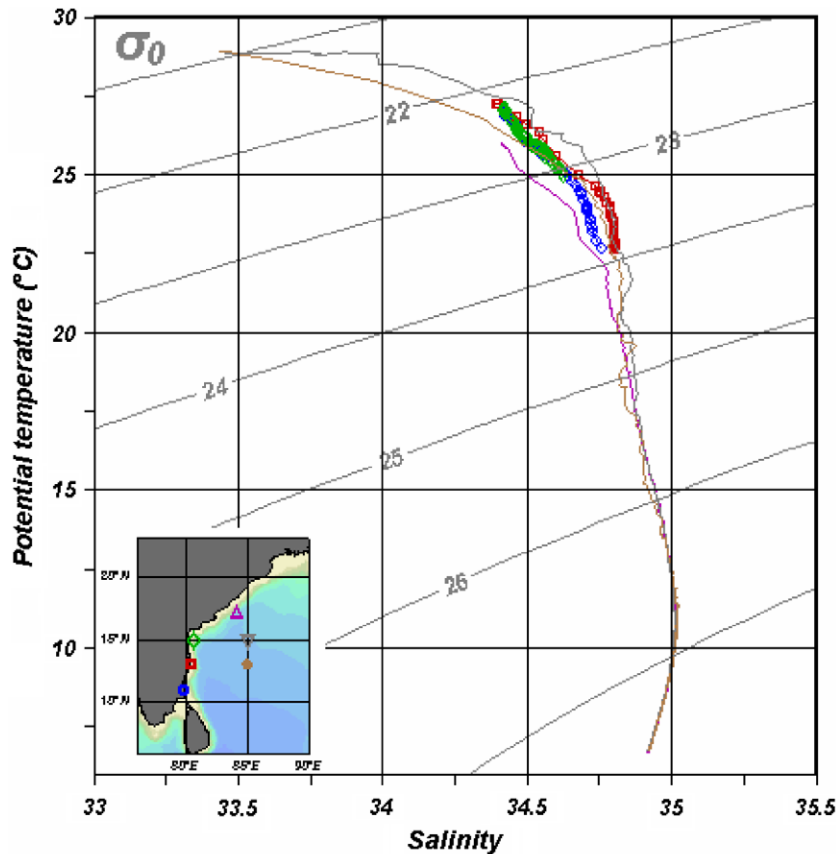


Fig. 2. T-S Diagram showing the variations in the water properties of Awarm gyre, cyclonic eddy and upwelling in the upper 300 m.

Water samples were collected using a Rosette sampler from standard depths down to 1000 m (surface, 10, 20, 30, 50, 75, 100, 150, 200, 300, 500, 750, 1000 m) and analysed for nitrate, nitrite, phosphate and silicate with a SKALAR auto-analyzer. Dissolved oxygen (DO) was estimated by Winkler's method. Chlorophyll *a* and primary productivity were measured at one coastal and one open ocean station on each transect. Water samples were collected from seven discrete depths according to the JGOFS protocols (UNESCO, 1994). Water samples for primary productivity were collected before sunrise and incubated *in situ* for 12 h after adding 1 ml of $\text{NaH}^{14}\text{CO}_3$ to each sample ($5 \mu\text{Ci}$ per 300 ml seawater). After incubation, the samples were filtered through 47 mm GF/F (pore size $0.7 \mu\text{m}$) filters under gentle suction, exposed to concentrated HCl fumes to remove excess inorganic carbon and kept in scintillation vials. Scintillation cocktail was added to the vials a day before the analysis, and the activity was counted in a Wallace scintillation counter. The Disintegrations per Minute (DPMs) values were converted into daily production rates ($\text{mg C m}^{-3} \text{ day}^{-1}$) using the formula of Strickland and Parsons (1972). For chlorophyll *a*, two liters of water from each depth were filtered through GF/F filters (pore size $0.7 \mu\text{m}$), and extracted with 10 ml of 90% acetone and analyzed spectrophotometrically (Perkin-Elmer UV/Vis). Column chlorophyll *a* (mg m^{-2}) and primary production ($\text{mg C m}^{-2} \text{ day}^{-1}$) were calculated by integrating the depth values.

Mesozooplankton was collected at all stations in the upper 300 m with a Hydrobios multiple plankton net (MPN) of 0.25 m^2 mouth area and mesh size $200 \mu\text{m}$. The nets of the MPN were open through depth ranges of surface-MLD, MLD-Thermocline (TB) and TB-300 m based on density and temperature profiles. Samples from each depth were sieved through $200 \mu\text{m}$ mesh, excess water removed by absorbent paper, and the displacement volume estimated (Harris et al., 2000). Zooplankton abundance was estimated by counting all the individuals present in the sample or the aliquot depending on the biovolume. All abundance data were converted to density (ind. m^{-3}) using the volume of water filtered by the net. Karl Pearson's (Product-

moment) correlation coefficient (r) was calculated between mesozooplankton biomass and density of each taxa present in the three different physical regions.

Data from the SeaWinds scatterometer on the QuikSCAT satellite were used to characterize the prevailing wind patterns (Freilich et al., 1994) and to estimate the upwelling (Ekman transport and Ekman pumping) along the western BoB during the study period, following Pickett and Paduan (2003). Merged altimetric data from NOAA (National Oceanic Atmospheric Administration) JASON-1/TOPEX/ERS-2/ENVISAT/GFO were used to analyse the Sea Surface Height Anomaly (SSHA). Surface geostrophic currents were computed from SSHA and compared with geostrophic currents derived from the CTD.

3. Results

The wind during the cruise (Fig. 3a) was predominantly south to southwesterly with an average speed of 8 m s^{-1} . There was a distinct change in wind direction from south–southwesterly to southwesterly–westerly at 15° N . The atmospheric pressure decreased toward the north from 1005 mb to 998 mb. Air temperature averaged 28° C and showed a diurnal cycle of $\pm 1^\circ \text{ C}$. Sea surface temperature (SST) was high ($>29.3^\circ \text{ C}$) in the central region of the BoB (Fig. 3a), but in coastal regions and at $17^\circ 30' \text{ N}$, $84^\circ 00' \text{ E}$ it was lower ($<27^\circ \text{ C}$). Surface Salinity (SS) was higher (>34) at coastal stations in the southern BoB than at offshore (<33.6) stations (Fig. 3b). In the northern BoB, the highest salinity was observed at $17^\circ 30'$; 84° E (Fig. 3b). Below 200 m salinity remained homogeneous around 35. The surface layer formed a cap of low salinity (<34), warm ($>29^\circ \text{ C}$) water in the area bounded by $13^\circ 30' \text{ N}$ to $15^\circ 30' \text{ N}$ and 82° E to 88° E , implying positive buoyancy, high dynamic height (*in situ*) and elevated (altimetric) sea-surface height (Fig. 4a and b). The greatest MLD (70 m) was observed in the central BoB that decreased toward the coast.

Meridional sections (4° away from the coast) of temperature, salinity and density in the upper 300 m (Fig. 5a) showed the isopleths sloping downward offshore from $13^\circ 30'$ to $15^\circ 30' \text{ N}$ with a vertical displacement of 50–100 m. In this section, MLD was deeper offshore (70 m) than coastal stations (20 m). The 15° C isotherm (Thermocline) dipped from $\approx 130 \text{ m}$ at the coastal station to $\sim 200 \text{ m}$ offshore.

The dissolved oxygen profile (Fig. 6a) showed variations in the oxygen minimum zone ($\sim 20 \mu\text{M}$ oxygen concentration) at the intermediate depths of both open ocean and coastal waters. The nitrate concentration (Fig. 6b) showed oligotrophic conditions ($<0.1 \mu\text{M}$) in the surface waters of the open ocean, whereas at the coastal stations the nitracline ($2 \mu\text{M}$) was lifted well into the surface layer. A similar distribution pattern was observed for phosphate concentrations (PO_4), with high values ($0.8 \mu\text{M}$) along the coastal and low values ($0.4 \mu\text{M}$) at the open ocean stations (Fig. 6c). Surface silicate (SiO_4) levels were $>4 \mu\text{M}$ throughout the region (Fig. 6d).

At the coastal stations, surface and water column chlorophyll *a* concentrations varied between 0.12 – 0.25 mg m^{-3} and 7.4 – 13.6 mg m^{-2} , respectively; whereas at the open ocean stations the ranges were 0.12 to 0.23 mg m^{-3} and 4.6 to 10.1 mg m^{-2} , respectively. The surface primary production in the BoB ranged from 2.59 to $9.23 \text{ mg C m}^{-3} \text{ day}^{-1}$ at the coastal stations and from 2.55 to $4.25 \text{ mg C m}^{-3} \text{ day}^{-1}$ in the open ocean waters. The integrated water column production levels at the coastal stations ranged from 108 to $357 \text{ mg C m}^{-2} \text{ day}^{-1}$ compared to 73 to $200 \text{ mg C m}^{-2} \text{ day}^{-1}$ at the oceanic stations.

Mesozooplankton standing stock was higher ($>1.2 \text{ ml m}^{-3}$) at the coastal stations (especially at $13^\circ 30' \text{ N}$ and $15^\circ 30' \text{ N}$) than at the open ocean stations (0.14 ml m^{-3}). Although the open oceanic regions were oligotrophic, at one station ($17^\circ 30' \text{ N}$, $84^\circ 00' \text{ E}$) in the cyclonic eddy of the northern BoB, mesozooplankton bio-volume was high (0.67 ml m^{-3}). Copepods were numerically the dominant group in all the samples. Other major groups encountered were larvae of decapods, chaetognaths, ostracods, euphausiids, amphipods, foraminifers, fish eggs and fish larvae.

3.1. Basin-scale process – warm gyre

The dynamic topography (Fig. 4a) computed at 10 m with respect to 1000 m showed a dynamic height of $>1.75 \text{ dyn m}$ in an area between $13^\circ 30'$ – $15^\circ 30' \text{ N}$ and 82° – 88° E . This clearly indicates that a clockwise circulation exists in this region. The calculated geostrophic velocity (Fig. 4a) was ~ 15 – 20 cm s^{-1} at the surface, characterized by a swirl of warm currents $>29^\circ \text{ C}$ in the central BoB. During this period, SSHA maps and

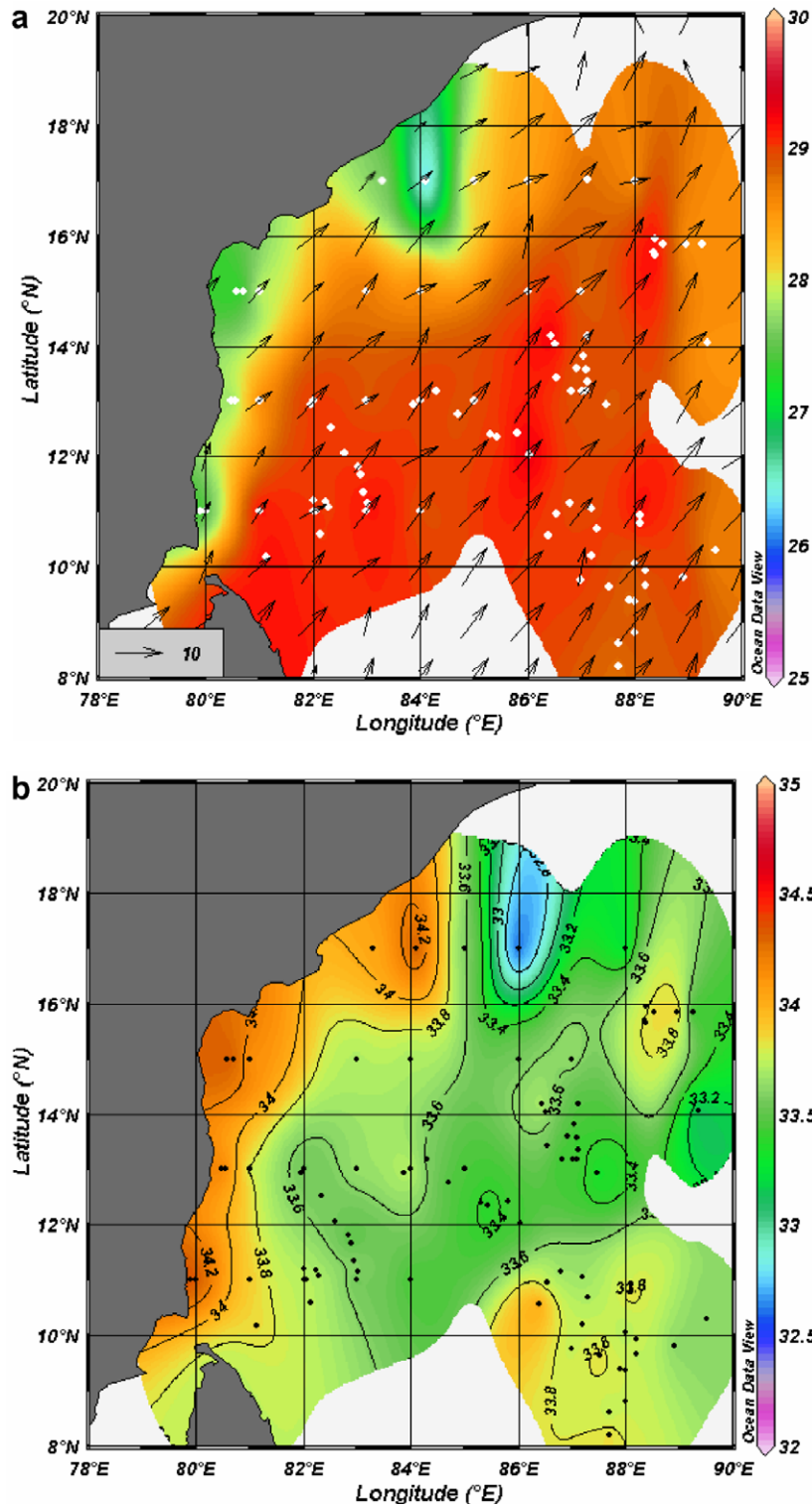


Fig. 3. (a) Surface distributions of temperature (*in situ*) overlaid with wind (QuikSCAT) during the sampling period are shown in the figure. High SST in the central BoB (warm gyre), low SST along the southeastern coast (upwelling) and lowest at 17°30' N; 84° E (cyclonic eddy) were identified. Southwesterly winds were predominant over the study region. (b) Surface distribution of salinity was high in the coastal areas and low in the open ocean regions; highest salinity was observed at 17°30' N; 84° E.

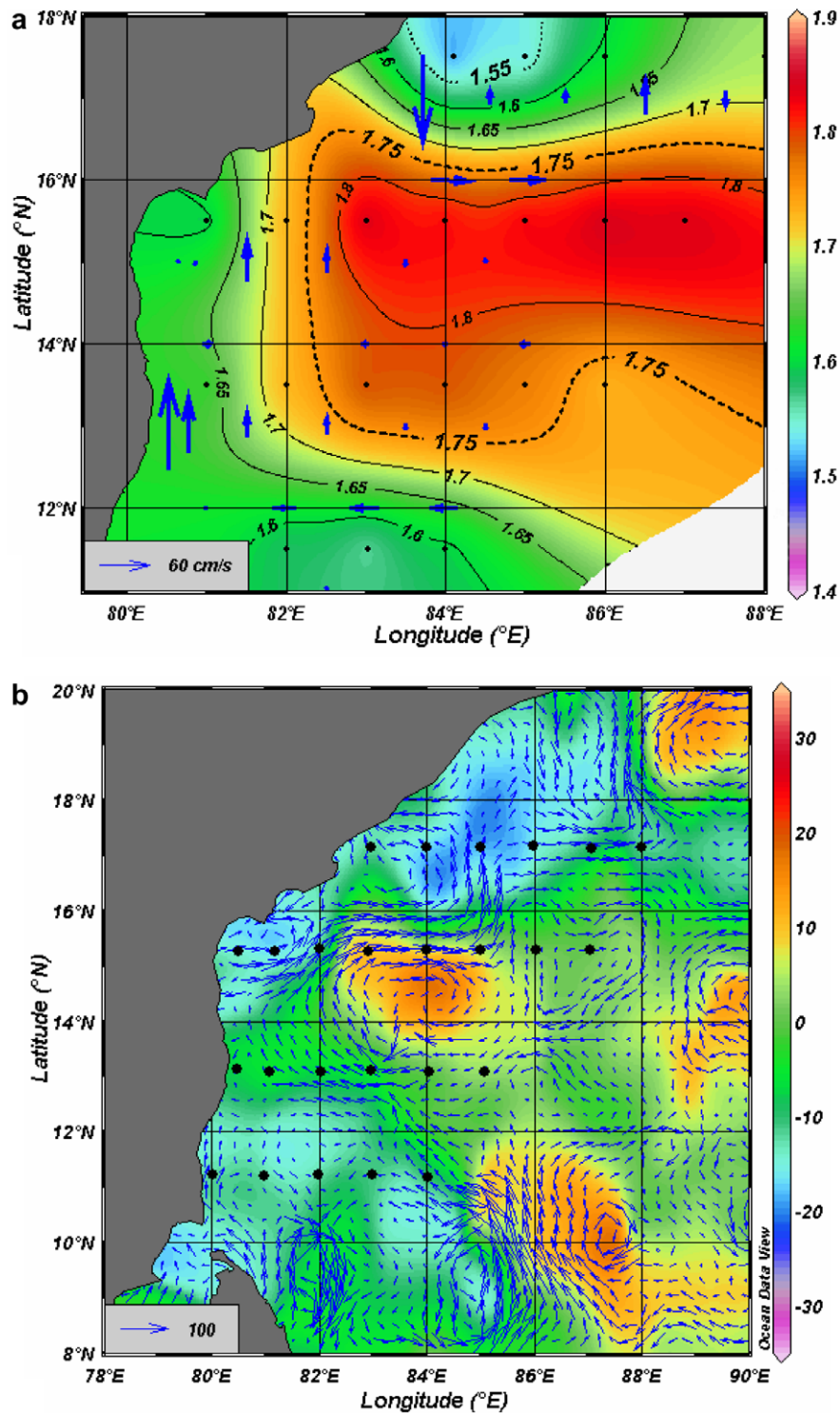


Fig. 4. (a) Dynamic height at 10 m w.r. to 1000 m is overlaid with geostrophic currents. Red colour indicates high, green low and blue least dynamic height (Scale at the right). Geostrophic current vectors show a clockwise circulation in the open ocean regions, anti-clockwise circulation centered at $17^{\circ}30' N$; $84^{\circ} E$ and a southerly movement along the southern coast. (b) Merged altimetric sea surface height anomaly (SSHA) from Jason-1, TOPEX, ERS-2, ENVISAT and GFO is overlaid with geostrophic currents from SSHA (High SSH in red and low in blue). Geostrophic current vectors indicate the circulation pattern.

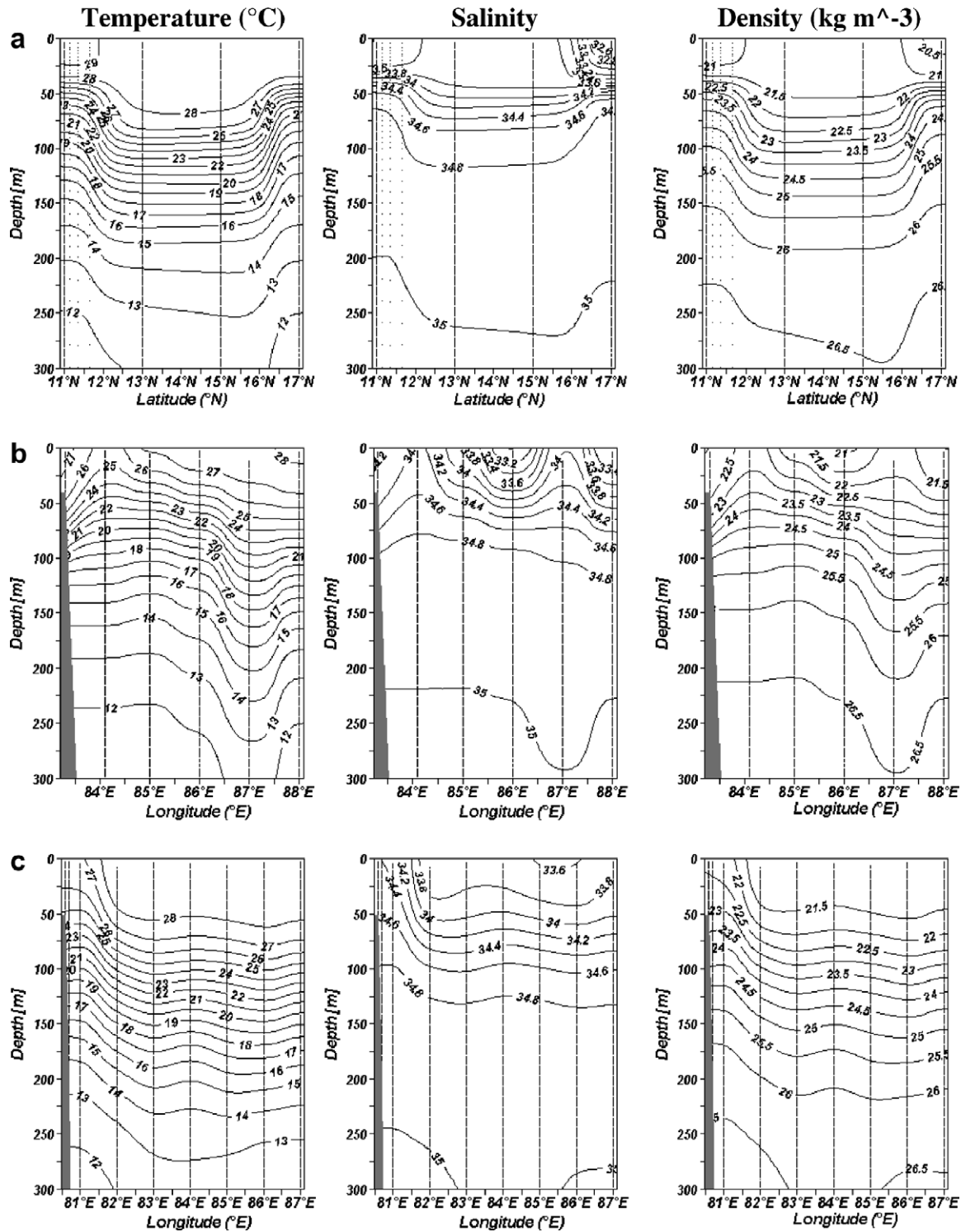


Fig. 5. Vertical sections of temperature ($^{\circ}\text{C}$), salinity and density (kg m^{-3}) in the upper 300 m of three physically distinct regions are plotted. (a) Warm gyre: meridional section was taken across the latitudes 4° away from the coast of each transect to provide a clear picture of down sloping of properties and the deep MLD generated by surface convergence. (b) Cyclonic eddy: a zonal section along $17^{\circ}30' \text{ N}$ clearly illustrates the doming up of the contours at 84° E . (c) Upwelling: a zonal section along $15^{\circ}30' \text{ N}$ indicates the upsloping of the contours across the shelf/slope region.

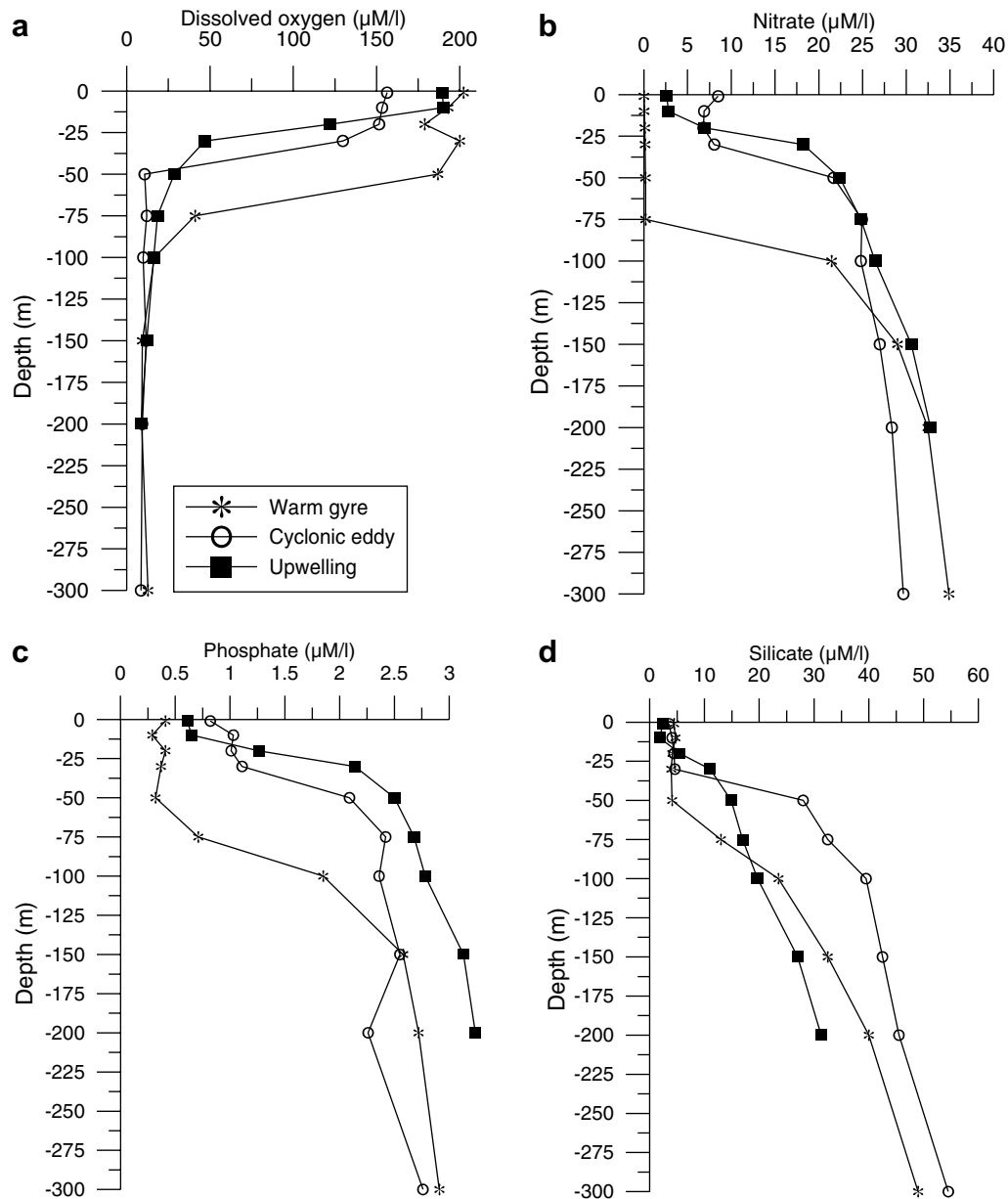


Fig. 6. Average concentration ($\mu\text{M/l}$) of (a) dissolved oxygen, (b) nitrate, (c) phosphate and (d) silicate in the three different hydrographic regimes.

computed geostrophic currents (Fig. 4b) from the merged altimetric data indicated the presence of a warm gyre in the central BoB. A homogeneous water column having a temperature of 28°C in the upper 70 m was observed in the warm gyre (Fig. 5a). Isopleths of temperature, salinity and density (Fig. 5a) were bowed down to depths of 50–100 m, increasing the thickness of the mixed layer. The warm (29°C), low salinity (~ 33.5) surface water resulted in sea level elevation of 5–15 cm in the central BoB above that of the peripheral region. In the warm gyre, dissolved oxygen remained saturated ($>200 \mu\text{M}$) and silicate concentrations were high ($>4 \mu\text{M}$), whereas nitrate ($0.1 \mu\text{M}$) and phosphate ($0.2 \mu\text{M}$) concentrations were very low (Fig. 6).

Average surface chlorophyll *a* (Fig. 7a) and primary production (Fig. 7b) in the warm gyre were 0.12 mg m^{-3} and $2.55 \text{ mg C m}^{-3} \text{ day}^{-1}$, respectively. Average integrated chlorophyll *a* and primary

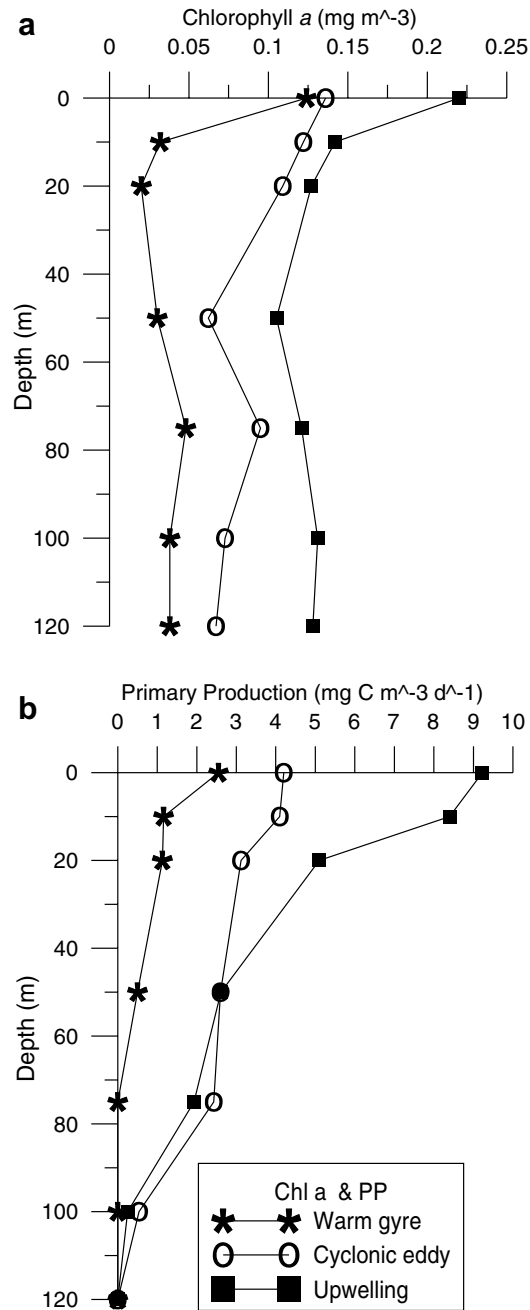


Fig. 7. Average vertical profiles of (a) chlorophyll *a* concentration (mg m^{-3}) and (b) primary productivity ($\text{mg C m}^{-3} \text{ day}^{-1}$) in the warm gyre, cyclonic eddy and upwelling regions.

production in the mixed layer (Fig. 8a) were 2.77 mg m^{-2} and $73 \text{ mg C m}^{-2} \text{ day}^{-1}$, respectively. The integrated chlorophyll *a* from the base of the mixed layer to 120 m (Fig. 8b) was low, 1.84 mg m^{-2} , while the primary production was barely discernible. Mesozooplankton biovolume (Fig. 9; Table 1) in the mixed layer of the warm gyre averaged 0.14 ml m^{-3} , which was much lower than in either the cyclonic eddy (0.67 ml m^{-3}) or the upwelling region (1.12 ml m^{-3}). Mesozooplankton biovolume decreased with depth (Fig. 10a; Table 1). Foraminifera, chaetognaths, copelates, siphonophores, fish larvae, and medusae, were the most prevalent taxa present in the warm gyre. Moreover, diurnal variation (Fig. 10a) was not significant in warm gyre. The average

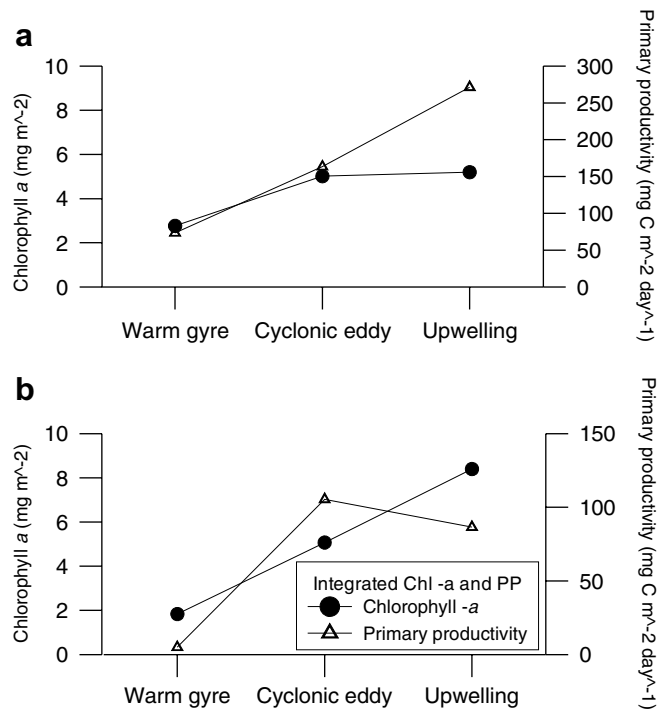


Fig. 8. Average integrated chlorophyll a (mg m^{-2}) and primary productivity ($\text{mg C m}^{-2} \text{day}^{-1}$) in the warm gyre, cyclonic eddy and upwelling region: (a) mixed layer and (b) mixed layer to 120 m. This depicts that the warm gyre is less productive than the other two regions and that production is negligible below the mixed layer.

population density of copepods was one-third of that observed in the upwelling region. The population density (Table 2) of foraminifera in the MLD of the warm gyre (4.72 ind. m^{-3}) was higher than in either the cyclonic eddy (negligible) or the upwelling region (0.23 ind. m^{-3}), indicating a higher ($r > 0.5$) affinity of this group to the warm waters (Fig. 11).

3.2. Mesoscale process – cyclonic eddy

Surface hydrological features showed cool ($<26.5 \text{ }^\circ\text{C}$) and high salinity waters (>34) in the northern BoB at $17^\circ30' \text{ N}$, 84° E (Fig. 3a and b). There was a low dynamic topography of 1.55 dyn m and negative SSHA of $<-15 \text{ cm}$, which we eventually identified as a cyclonic eddy. The geostrophic currents (Fig. 4a and b) computed from *in situ* and altimetric observations are anti-clockwise with low temperature ($27 \text{ }^\circ\text{C}$) at the eddy centre. The isopleths of temperature, salinity and density domed toward the surface (Fig. 5b), reducing the depth of the mixed layer to 38 m and that of the thermocline to 137 m. The isopycnals ($25\sigma_t$ level) rose from 70 m to 20 m, indicating that subsurface water was moving toward the surface. Dissolved oxygen concentrations (Fig. 6a) were low ($\approx 164 \text{ } \mu\text{M}$), and nutrient concentrations (Fig. 6b–d) were high ($\text{NO}_3 \sim 8.2 \text{ } \mu\text{M}$, $\text{PO}_4 \sim 0.9 \text{ } \mu\text{M}$ and $\text{SiO}_4 \sim 4.1 \text{ } \mu\text{M}$) in the mixed layer, which indicated the presence of the cyclonic eddy. Average surface chlorophyll a and primary production (Fig. 7a and b) in the cyclonic eddy region were 0.14 mg m^{-3} and $4.2 \text{ mg C m}^{-3} \text{day}^{-1}$, respectively. The average values of integrated chlorophyll a and primary production in the mixed layer were 5.01 mg m^{-2} and $163 \text{ mg C m}^{-2} \text{day}^{-1}$, respectively (Fig. 8a). From the base of the MLD to 120 m, these values were 5.07 mg m^{-2} and $105 \text{ mg C m}^{-2} \text{day}^{-1}$, respectively (Fig. 8b). The mesozooplankton biovolume (Fig. 9) in the MLD of the eddy averaged 0.67 ml m^{-3} , and from the base of the MLD to thermocline and from the thermocline to 300 m, it gradually decreased from 0.26 ml m^{-3} to 0.02 ml m^{-3} (Table 1). The numerical density of the dominant groups of zooplankton in this region varied: Copepoda (1036 ind. m^{-3}), Ostracoda (13 ind. m^{-3}), Decapoda (21 ind. m^{-3}), euphausiids (6 ind. m^{-3}), Chaetognatha (32 ind. m^{-3}), fish eggs (216 ind. m^{-3}) and fish larvae (1 ind. m^{-3}) (Table 2). Mesozooplankton

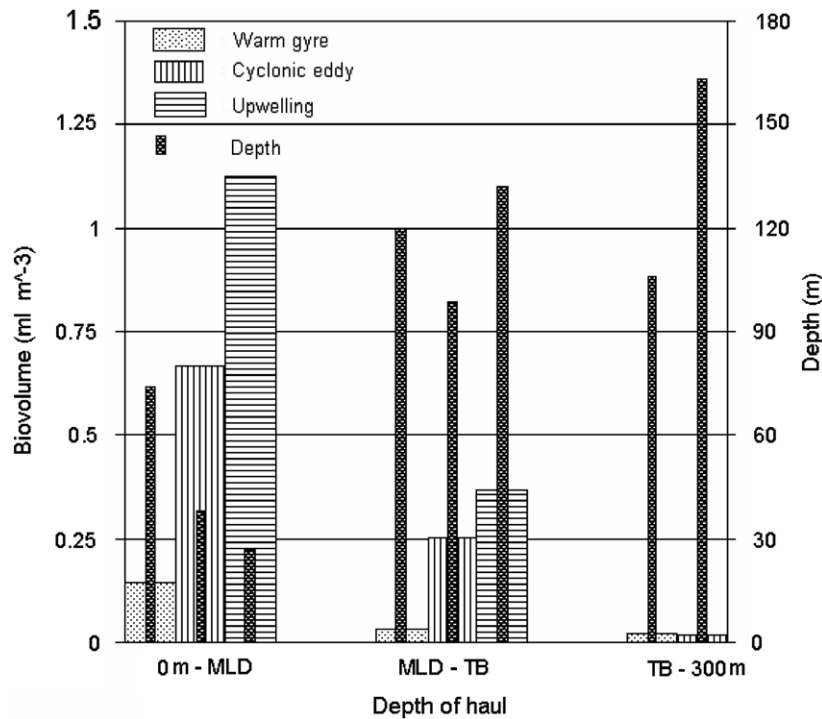


Fig. 9. Average mesozooplankton biovolume (ml m^{-3}) in the mixed layer, thermocline (TB) and TB to 300 m of the warm gyre, cyclonic eddy and upwelling region. The secondary axis shows the average distance (m) hauled by the MPN net according to the above criteria. High biovolume was observed in the upwelling region even though the MLD was very shallow, while least biovolume was observed in the warm gyre region where the MLD was the highest.

in the mixed layer exhibited diurnal fluctuation, with higher biovolume observed during the day than at night, (Fig. 10b). Population density in the cyclonic eddy showed significant correlations ($r > 0.5$) of the following taxa: fish eggs, fish larvae, Decapoda, Amphipoda, doliolids, Gastropoda, Heteropoda and Pteropoda (Fig. 11).

3.3. Wind driven process – coastal upwelling

The coastal regions experience persistent winds (south–southwesterly) with an average speed about 8 m s^{-1} (Fig. 3a). The notable feature was a shift in the wind direction from south–southwest to westerly at 15° N . The SST (Fig. 3a) along the coast was $\sim 27.5^\circ \text{ C}$, which was 1.5° C cooler than the offshore stations, whereas surface salinity (Fig. 3b) was > 34 , which was ~ 0.6 more saline than the oceanic water. The shallow mixed layer of $< 27 \text{ m}$ and thermocline depth of $< 159 \text{ m}$, together with the low dynamic topography of $< 1.6 \text{ dyn m}$ and SSHA of $< -5 \text{ cm}$, illustrated the cooling of surface water as a result of upwelling (Fig. 4a and b). Upward slope of the isopleths of temperature, salinity and density (Fig. 5c) toward the shelf indicated coastal upwelling was occurring in the southern BoB ($11^\circ 30' - 15^\circ 30' \text{ N}$). This region was also characterised by moderately low dissolved oxygen ($> 190 \mu\text{M}$) and high concentrations of NO_3 ($\sim 2.5 \mu\text{M}$), PO_4 ($\sim 0.6 \mu\text{M}$) and SiO_4 ($\sim 3 \mu\text{M}$) (Fig. 6a–d). Compared to the warm gyre and cyclonic eddy, the upwelling region showed high surface chlorophyll *a* and primary production (0.25 mg m^{-3} and $9.23 \text{ mg C m}^{-3} \text{ day}^{-1}$, respectively) (Fig. 7a and b). Similarly, the average values of integrated chlorophyll *a* and primary production in the MLD (Fig. 8a) were remarkably high (5.2 mg m^{-2} and $271 \text{ mg C m}^{-2} \text{ day}^{-1}$, respectively). Average, integrated chlorophyll *a* and primary production from the base of mixed layer to 120 m were 8.4 mg m^{-2} and $87 \text{ mg C m}^{-2} \text{ day}^{-1}$, respectively (Fig. 8b). The mesozooplankton biovolume, (Fig. 9) averaging 1.12 ml m^{-3} in the mixed layer was the highest observed (Table 1). The biovolume in the thermocline (0.37 ml m^{-3}) was also higher than that observed in the cyclonic eddy (0.26 ml m^{-3}) or warm-gyre (0.03 ml m^{-3}) regions. Although the MLD

Table 1
 Characteristics of various parameters (range of temperature, salinity, depth of MLD/TB, dissolved oxygen, nitrate, phosphate, silicate and the mean values of chlorophyll *a*, primary productivity and Meso zooplankton biovolume) in the three different hydrographic regimes

Processes	Depth zone	Depth (m)	Temp. (°C)	Sal.	DO (µM/l)	NO ₃ (µM/l)	PO ₄ (µM/l)	SiO ₄ (µM/l)	Chl <i>a</i>		PP		Biovolume (ml m ⁻³)
									Sur. (mg m ⁻³)	Col. ^a (mg m ⁻²)	Sur. (mg C m ⁻³ d ⁻¹)	Col. ^a (mg C m ⁻² d ⁻¹)	
Warm gyre	MLD	74	28.86–28.70	33.56–33.76	202–187	0.01–0.18	0.4–0.71	4.45–4.1	0.12	2.77	2.55	73	0.14
	TB	194	28.70–15.00	33.76–34.94	186–9.3	0.18–29	0.71–2.58	4.12–32.5	—	1.84	—	Negligible	0.034
	300	300	15.00–11.79	34.94–35.12	9–8.5	29–34.89	2.58–2.91	32.5–49	—	4.61	—	73	0.025
Cyclonic eddy	MLD	38	26.82–26.39	34.10–34.18	156–152	8.5–8.06	0.82–1.1	3.5–4.6	0.14	5.01	4.2	163	0.67
	TB	137	26.39–15.00	34.18–34.94	151–9.9	8.06–21.7	1.112.36	4.6–39.5	—	5.07	—	105	0.26
	300	300	15.00–11.28	34.94–35.01	9.9–8	21.78–29.68	2.362.76	39.5–54	—	10.08	—	268	0.02
Upwelling	MLD	27	27.37–26.82	34.30–34.41	189–122	2.62–2.8	0.61–1.26	2.4–5.5	0.25	5.2	9.23	271	1.12
	TB	159	26.88–15.00	34.39–34.94	122–12	2.8–6.95	1.263.13	5.5–27	—	8.4	—	87	0.37
										13.6		358	

^a Column values were integrated from surface to mixed layer, mixed layer to 120 m and surface to 120 m.

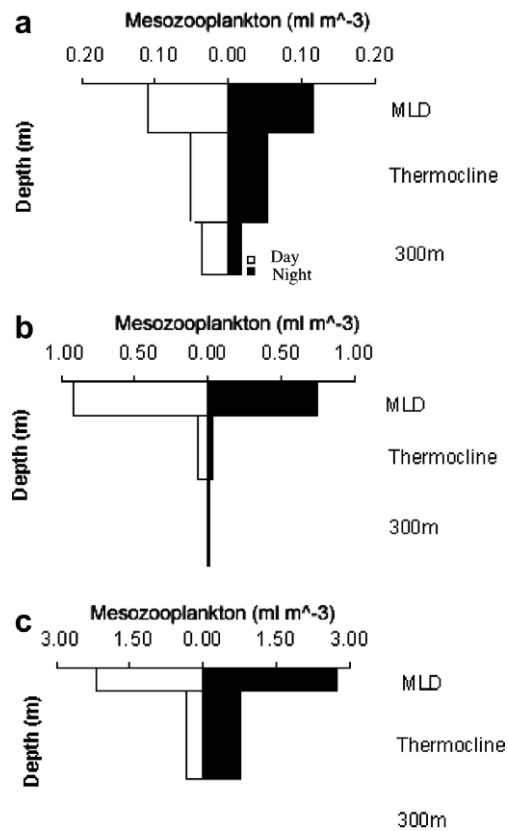


Fig. 10. Average diurnal variation of mesozooplankton biovolume ml m^{-3} in (a) the warm gyre, (b) the cyclonic eddy and (c) the upwelling region. The width of each depth stratum is proportional to the distance of net hauling.

(~ 27 m) was very shallow, mesozooplankton abundance was maximum and diverse, too (Figs. 9 and 11). The dominant taxa were Copepoda (1697 ind. m^{-3}), Copelata (291 ind. m^{-3}), Ostracoda (42 ind. m^{-3}), Chaetognatha (37 ind. m^{-3}), doliolids (33 ind. m^{-3}), euphausiids (27 ind. m^{-3}), Decapoda (22 ind. m^{-3}), Polychaeta (16 ind. m^{-3}), pteropods (14 ind. m^{-3}), siphonophores (10 ind. m^{-3}), medusae (6 ind. m^{-3}), salps (1 ind. m^{-3}), Gastropoda (1 ind. m^{-3}) and Amphipoda (1 ind. m^{-3}) in decreasing order of abundance. Fish eggs (617 ind. m^{-3}) and larvae (2 ind. m^{-3}) were more abundant in the upwelling region than in either the warm gyre or the cyclonic eddy (Table 2). The diurnal variation in the MLD and in the thermocline layers was only marginal (Fig. 10c).

4. Discussion

Basin-scale and mesoscale physical forcing influences the spatial heterogeneity of biological production in marine ecosystems (Pakhomov and Perissinotto, 1997; Huskin et al., 2001). Physical processes such as gyres, eddies and upwelling increase or decrease the nutrients in the upper layers of the ocean and hence, organize the biological production. The physical influences on the structure of the plankton communities are complex at several spatial and temporal scales. The variability of biological production and its transfer to the higher trophic levels as a result of the influence exerted by these physical processes are explained further.

4.1. Warm gyre and biological production

During the summer monsoon, the central BoB showed the existence of the warm gyre that formed in the spring inter-monsoon. We may look at the dynamics that favour the existence of the warm gyre by analyzing

Table 2
 General taxonomic composition of mesozooplankton and its mean abundance (ind. m⁻³) in the upper 300 m of three different physical systems: the warm gyre, the cyclonic eddy and coastal upwelling

Meso-Zooplankton groups	Warm gyre		Cyclonic eddy		Upwelling	
	MLD 0–74 m	Thermocline 74–194 m	MLD 0–38 m	Thermocline 38–137 m	MLD 0–27 m	Thermocline 27–159 m
Foraminifera	4.72	1.88	0.00	0.36	0.23	0.00
Medusa	0.28	0.01	2.94	3.27	5.75	0.44
Siphonophora	6.53	0.41	5.94	0.26	9.73	1.30
Anthozoa	0.00	0.00	0.03	0.01	0.23	0.00
Ctenophora	0.00	0.00	0.00	4.02	0.56	0.01
Polychaeta	1.71	0.67	5.42	3.15	15.53	3.48
Pteropoda	0.87	0.09	1.91	0.01	14.30	0.42
Heteropoda	0.04	0.00	0.04	0.00	0.00	0.01
Gastropoda	0.34	0.10	0.03	0.00	1.23	0.83
Cephalopoda	0.09	0.01	0.00	0.00	0.17	0.04
Ostracoda	13.09	5.57	13.63	2.45	42.11	14.85
Copepoda	310.10	64.83	1036	99.22	1697.33	446.99
Isopoda	0.00	0.00	0.00	0.00	1.34	0.00
Amphipoda	0.97	0.13	0.99	0.07	0.90	0.08
Euphausiid	1.43	0.74	6.29	0.38	26.55	12.28
Decapoda	1.63	0.65	21.57	0.19	21.25	3.51
Stomatopod	0.00	0.00	0.52	0.00	0.88	0.06
Chaetognatha	24.47	3.83	32.42	1.00	37.96	15.25
Copelata	10.75	0.10	16.38	0.00	291.14	6.30
Salpa	0.08	0.02	0.04	0.01	1.39	0.27
Doliolida	0.40	0.12	0.55	0.21	33.19	3.31
Fish egg	0.07	0.01	216.99	0.00	616.84	21.02

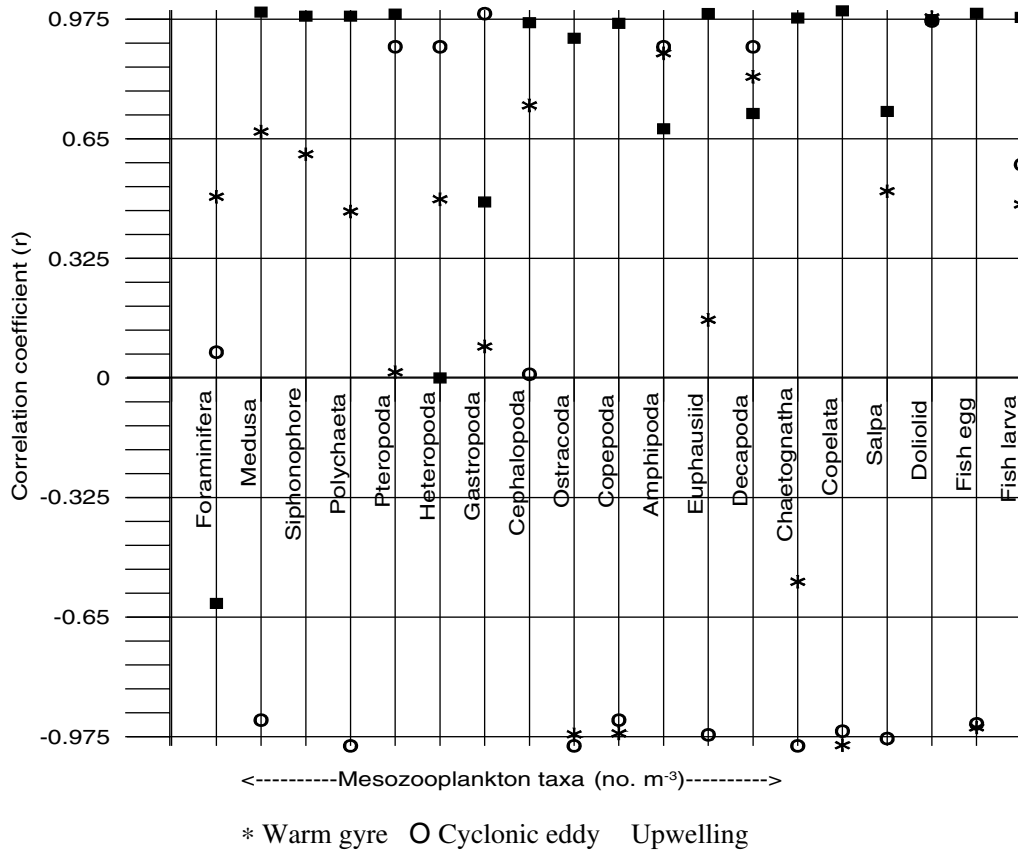


Fig. 11. Correlation coefficient (r) between average mesozooplankton biovolume (ml m^{-3}) and abundance of each taxon (ind. m^{-3}) in the upper 300 m of each station of the warm gyre, the cyclonic eddy and the upwelling region. This indicates the degree of affinity of each taxon to the respective environments.

the wind stress curl and current patterns. Negative wind stress curl over the central BoB during the summer monsoon promotes convergence of warm surface water and elevated SSH. The northward moving western boundary current (WBC) merges with the southward moving freshwater plume at 16°N and turns offshore. Part of this offshore deflection meanders through the open ocean and recirculates towards the coastal region at around 12°N , forming a clockwise circulation in the central BoB (Fig. 4a and b). High dynamic topography of $>175 \text{ cm}$ (Fig. 4a) extending across the region (12°N – 16°N and 82°E – 86°E) suggests convergence of warm and less saline surface water as a result of the clockwise circulation. The surface currents derived from the altimetric data were in good agreement with the surface observations (Fig. 4b). In the warm gyre region, the isopycnals were bowed down because of the clockwise circulation, deepening the MLD to $>70 \text{ m}$ and the thermocline to $>190 \text{ m}$ (Fig. 5a). The freshwater-induced stratification impedes the advection of nutrients in to the euphotic zone, leading to the development of oligotrophic conditions in the BoB (Prasannakumar et al., 2002). Consequently, the waters of the warm gyre were characterised by high dissolved oxygen concentrations ($>190 \mu\text{M}$; Fig. 6a) and low nutrients ($\text{NO}_3 < 0.1 \mu\text{M}$, $\text{PO}_4 < 0.5 \mu\text{M}$, $\text{SiO}_4 < 4 \mu\text{M}$; Fig. 6b–d). The nutrient fluxes in the euphotic zone of the warm gyre are mainly determined by the steepness of the density gradient; steeper gradients more intensely retard the upward nutrient flux to the surface. As expected, our results showed very low concentrations of chlorophyll a and primary production in the warm gyre compared to other regions, despite the cloud cover over the central BoB being only four octa. Thus, it is assumed that the biological production is nutrient limited, because the nutricline lies much deeper than the base of the euphotic zone. Highly stratified, oligotrophic open oceans are nutrient depleted and sustain mostly regenerated production dominated by pico- and nanoplankton. The reduced phytoplankton production in warm gyre, in turn

results in the subsequent decline of the mesozooplankton biovolume (0.14 ml m^{-3}) (Fig. 9). However, this favours some components of the zooplankton community; the maximum abundance of Foraminifera (4.72 ind. m^{-3}) was observed in the warm gyre (compared to the cyclonic eddy, 0.01 ind. m^{-3} and the upwelling region, 0.23 ind. m^{-3}). The assemblage of planktonic Foraminifera is dependant on the depth of the thermohaline, light intensity and food availability in the euphotic zone (Kuroyanagi et al., 2002). The two dominant species encountered in this study, *G. ruber* and *G. sacculifer* contain symbiotic algae, and hence may thrive well in oligotrophic, warm and stratified conditions (Gastrich, 1987; Thunell and Reynolds, 1984), explaining the clear affinity of foraminifers for the warm oligotrophic waters of the BoB during the summer monsoon (Gupta et al., 1997). The absence of diurnal variation (Fig. 10a) in zooplankton biovolume and abundance indicates that there is insignificant vertical movement of the zooplankton community. This may be a result of the vertical gradients being too steep for the species to cross, or because the physiological cost of undertaking the migrations is too high in such a low productivity environment, or because there is a lack of predation pressure by visually hunting carnivores.

4.2. Cyclonic eddy and biological production

The second hydrological process in the BoB detected both by the altimetric SSHa and geostrophic currents during the summer monsoon, was an anticlockwise circulation centered at $17^{\circ}30' \text{ N}$, 84° E . This eddy centre was characterised by a temperature $<26.5^{\circ} \text{ C}$ and more a saline water of >34 relative to its peripheral regions (Fig. 3a and b). Babu et al. (1991) documented the presence of a cyclonic eddy off Visakhapattanam (18° N) during the southwest monsoon of 1984. A possible mechanism leading to the formation of such a cyclonic eddy is the baroclinic instability developed at the interface of two opposing currents (freshwater plume and Western Boundary Current) that occur along the margin of the western boundary of the BoB. Wind stress curl computation over these regions yields positive values favouring the formation of a cyclonic eddy. The dynamic topography (Fig. 4a) revealed that there was an anticlockwise circulation with cool water centered at $17^{\circ}30' \text{ N}$, 84° E . The cyclonic eddy was characterised by doming of the temperature, salinity and nutrient isopleths coming to the surface, indicating there was upwelling of deeper waters associated with this process (Fig. 5b). Sufficient nutrients have been supplied ($\text{NO}_3 > 7 \mu\text{M}$, $\text{PO}_4 > 0.8 \mu\text{M}$, $\text{SiO}_4 > 3.5 \mu\text{M}$) to the surface layer (Fig. 6b–d) to switch conditions from oligotrophy to eutrophy. Under normal conditions cyclonic eddies result in enhanced surface primary production and elevated concentrations of chlorophyll in the open ocean (McGillicuddy and Robinson, 1997; Martin and Richards, 2001; Falkowski et al., 1991). However, despite the nutrient levels in the BoB cyclonic eddy being higher than in the upwelling regions, the chlorophyll (Chl *a*) and primary production (Fig. 7a and b) were not so high as in the upwelling zones. A number of factors may be contributing to this unexpected result: (1) Reduced solar irradiance resulting from the heavy cloud cover over this region; (2) as in other high-nutrient, low chlorophyll (HNLC) regions, the low availability of iron may be limiting primary production, especially by diatoms; which would normally bloom in such high silicate conditions; (3) poor nutrient utilization by the impoverished phytoplankton community due to intense grazing of mesozooplankton; and (4) replacement of ‘regenerated production’ by ‘new production’. Prasannakumar et al. (2004) reported low production in the nutrient-enriched regions (cyclonic eddy) of the northern BoB due to the lack of sufficient light for photosynthesis. But during our observational period, cloud cover was only 4 octa, and so solar irradiance would not have been a limiting factor. High riverine influx brings sufficient iron into the BoB. Rejomon (2006) reported that the amount of dissolved iron in the upper layers of the BoB varies from 2.3 to 2.7 ppb. It may be noted that the deep waters of the BoB contain plenty of regenerated iron, and iron concentrations in the Indian Ocean are generally high (GEOSECS data). Thus, it is unlikely that iron is a limiting factor for phytoplankton growth in the BoB. In the cyclonic eddy, the mesozooplankton biovolume was relatively lower than in the upwelling region. Therefore, the grazing pressure of mesozooplankton on phytoplankton is not likely the reason for poor utilization of nutrients and low production. Although the environment in the cyclonic eddy was more favourable for high production ($\text{NO}_3 - 8.5 \mu\text{M}$) than in the upwelling region ($\text{NO}_3 - 2.6 \mu\text{M}$), the most plausible mechanism that might have limited the biological production (Fig. 7a and b; Table 1) was the switching over from the previously sustained ‘regenerated production’ to ‘new production’. Regenerated production utilizing ammonia as a source of nitrogen normally occurs in the stratified open ocean. During the cyclonic eddy formation, nitrate from the deeper waters is brought to

the surface. As a result, the phytoplankton community that is adapted to the oligotrophic stratified open ocean has to switch slowly over to a new community that can directly utilize the abundant nitrate (new production). Therefore, switching over from 'regenerated production' to 'new production' takes a longer time, as it requires the establishment of the new community. Thus, the available nitrate remained unutilized leading to low biological productivity. The mesozooplankton biovolume (0.67 ml m^{-3}) in the cyclonic eddy was only half that observed in the upwelling region (1.12 ml m^{-3}), but fourfold higher than that of the warm gyre (0.14 ml m^{-3}). Diversity of the zooplankton taxa (Fig. 11) in the cyclonic eddy were also less fewer to the upwelling region, but the density of fish eggs ($\approx 215 \text{ no. m}^{-3}$) and larvae ($\approx 2 \text{ ind. m}^{-3}$) were greater in the cyclonic eddy than in the warm gyre. To sum up, the biological production and energy transfer observed in the cyclonic eddy were higher than in warm gyre, but lower than in upwelling region.

4.3. Upwelling and biological production

The upwelling along the coastal regions of the southern BoB extends from $13^{\circ}30' \text{ N}$ to $15^{\circ}30' \text{ E}$. The prevailing winds (Fig. 3a) over the coastal regions were predominantly south to southwesterly with an average speed of 8 m s^{-1} and were favourable for the development of offshore Ekman transport and hence upwelling. The continental shelf along the eastern margin of India is narrow ($\sim 40 \text{ km}$), and therefore the upwelling is restricted to a narrow band (Qasim, 1977). Ekman pumping from wind stress curl is reported to be as important as Ekman transport forced by the alongshore winds (Pickett and Paduan, 2003). Shetye et al. (1991) documented an Ekman transport of $120 \text{ m}^3 \text{ s}^{-1}$ per 100 m during the summer monsoon in the BoB. Ekman transport ($> 3 \times 10^3 \text{ kg m}^{-1} \text{ s}^{-1}$) and volume transport ($> 300 \text{ m}^3 \text{ s}^{-1}$ per 100 m) along the coastal stations computed from QuikSCAT wind suggest an offshore divergence of surface waters, supporting the upwelling. Gopalakrishna and Sastry (1985) argued that the intensity of upwelling along the east coast of India is reduced by the equatorward flow of low salinity water, which overcompensates the offshore Ekman transport. In our study it was clear that northward moving western boundary currents and southward moving freshwater plume (strong gradient in the thermohaline structure) combine at 16° N and move offshore. Such an offshore movement will prevent intrusion of the low salinity waters from the north along the coast in the south of the BoB. The wind forced the surface waters to diverge offshore, bringing cool waters (27° C) into the surface and lowering the sea level by $5\text{--}15 \text{ cm}$ (Fig. 4b). Surface geostrophic currents and a negative SSH of -5 to -15 cm (Fig. 4a) indicated the presence of very weak Western Boundary Currents flowing northward. The upward sloping of the isolines of temperature, salinity and density (Fig. 5c) across the shelf resulted in nutrient replenishment ($\text{NO}_3 \sim 2.5 \mu\text{M}$, $\text{PO}_4 \sim 0.6 \mu\text{M}$, $\text{SiO}_4 \sim 4 \mu\text{M}$) of the surface layers. Upsloping of the isopycnals and nutricline (Fig. 6b–d) ($\approx 6\text{--}20 \mu\text{M NO}_3$ at $20\text{--}30 \text{ m}$) to the surface, and availability of sufficient solar irradiance resulted maximum biological production. The higher dissolved oxygen ($185 \mu\text{M}$) concentration in the mixed layer of the upwelling region, compared to that in the cyclonic eddy (Fig. 6a), might have resulted from high photosynthetic activity. The nutrient enrichment of the surface waters stimulated phytoplankton growth, thereby enhancing the surface chlorophyll *a* concentrations and primary production to $> 0.24 \text{ mg m}^{-3}$ and $> 9.8 \text{ mg C m}^{-3} \text{ day}^{-1}$, respectively (Fig. 7a and b). The integrated chlorophyll and primary production observed (Fig. 8a) in the mixed layer and mixed layer to 120 m (Fig. 8b; Table 1) were double those in the cyclonic eddy. Further, the nutrient concentrations were halved in the upwelling region ($\text{NO}_3 \sim 3 \mu\text{M}$), relative to those in the cyclonic eddy ($\text{NO}_3 \sim 7 \mu\text{M}$). Even though both systems (upwelling and cyclonic eddy) are divergent, reduction of nutrient concentrations, higher biological production and its efficient transfer to higher trophic levels show that the turnover rates are higher in the coastal ecosystem (upwelling) than in the oceanic system (cyclonic eddy). The coastal regions receive inputs of nutrients via the riverine outflows and runoff from the land inputs, which sustain 'new production'. So coastal regions can respond rapidly to episodic events like upwelling. Since production in the upwelling region is more predominantly 'new production', the phytoplankton community can respond faster to favourable events and the biological transfer to higher trophic levels is always higher. Diel variation in mesozooplankton standing stock was insignificant in the upwelling region because there was high availability of food at all depths (Fig. 10). Most abundant taxa were copepods, ostracods, euphausiids, decapods, and gelatinous groups like siphonophores, medusae, and chaetognaths. Fish eggs and larvae were also abundant in this region that offers a highly favourable environment for growth and development of fish. According to an optimal environmental window concept (Cury and Roy,

1989), reproductive success in fishes is maximised under moderate upwelling conditions, because the larvae can maintain themselves in the patches of abundant food supply. According to the trophic pathway classification proposed by Legendre and Rassoulzadegan (1996), the situation observed in the coastal upwelling would correspond mostly to an herbivorous food web and there are very few steps in the carbon transfer to higher trophic levels, implying a highly efficient energy transfer. Basin-scale and mesoscale processes influenced not only the primary production, but also the planktonic distribution and migrations. Thus, the secondary producers attract higher trophic level organisms like fishes. All these results lead to the conclusion that zooplankton populations within the various hydrographic regimes of the BoB change markedly in response to the differing ecological regimes created by the contrasting hydrographic processes - upwelling, cyclonic eddy and warm gyre.

Acknowledgements

We thank Dr. S.R Shetye, Director, National Institute of Oceanography, Goa and the Director, Centre for Marine Living Resources and Ecology, Kochi for providing facilities for the study. We are grateful to Dr. K. Banse, School of Oceanography, University of Washington, Seattle, USA and Dr. M.V. Angel, Southampton Oceanographic Centre, UK for critically reading the manuscript and offering valuable suggestions. We are also thankful to all the participants of Cruise No. 215 of FORV Sagar Sampada for the help rendered in sampling. This investigation was carried out under the MR-LR programme funded by Department of Ocean Development, Govt. of India, New Delhi and is the contribution of the National Institute of Oceanography, Goa.

References

- Achuthankutty, C.T., Madhupratap, M., Nair, V.R., Nair, S.R.S., Rao, T.S.S., 1980. Zooplankton biomass and composition in the western Bay of Bengal during late southwest monsoon. *Indian Journal of Marine Sciences* 9, 201–206.
- Babu, M.T., PrasannaKumar, S., Rao, D.P., 1991. A subsurface cyclonic eddy in the Bay of Bengal. *Journal of Marine Research* 49, 403–410.
- Bhavanarayana, P.V., La Fond, E.C., 1957. On the replenishment of some plant nutrients during the upwelling period on the East coast off India. *Indian Journal of Fisheries* 4, 75.
- Cury, P., Roy, C., 1989. Optimal environmental window and pelagic fish recruitment success in upwelling areas. *Canadian Journal of Fisheries and Aquatic Sciences* 46, 670–680.
- Falkowski, P.G., Ziemann, D., Kolber, D., Biefalg, P.K., 1991. Role of eddy pumping in enhancing primary production in the ocean. *Nature* 352, 55–58.
- Freilich, M.H., Long, D.G., Spencer, M.W., 1994. Sea winds: a scanning scatterometer for ADEOS II – Science overview. In: *Proceedings of the International Geosciences Remote Sensing Symposium, Pasadena, CA*, pp. 960–963.
- Gastrieh, M.D., 1987. Ultrastructure of a new intracellular symbiotic alga found within planktonic foraminifera. *Journal of Phycology* 23, 132–623.
- Gill, A.E., 1982. *Atmosphere – Ocean Dynamics*. Academic press, New York, p. 662.
- Gomes, H., Goes, J.I., Saino, T., 2000. Influence of physical processes and freshwater discharge on the seasonality of phytoplankton regime in the Bay of Bengal. *Continental Shelf Research* 20, 313–330.
- Gopalakrishna, V.V., Sastry, J.S., 1985. Surface circulation over the shelf off the east coast of India during southwest monsoon. *Indian Journal of Marine Sciences* 14, 62–65.
- Gupta, M.V.S., Curry, W.B., Ittekkot, V., Muralinath, A.S., 1997. Seasonal variation in the flux of planktonic foraminifera: sediment trap results from the Bay of Bengal, Northern Indian Ocean. *Journal of Foraminiferal Research* 27, 5–19.
- Harris, R.P., Wiebe, P.H., Lenz, J., Skjoldal, H.R., Huntley, M., 2000. *ICES Zooplankton Methodology Manual*. Academic Press, Sandiego, CA, pp. 87–89.
- Huskin, I., Anadon, R., Medina, G., 2001. Mesozooplankton distribution and copepod grazing in the subtropical Atlantic near the Azores: influence of mesoscale structures. *Journal of Plankton Research* 23, 671–691.
- Kuroyanagi, A., Kawahata, H., Nishi, H., Honda, C.M., 2002. Seasonal changes in planktonic foraminifera in the North-western North Pacific Ocean: sediment trap experiments from subarctic and subtropical gyres. *Deep Sea Research II* 49, 5627–5645.
- LaFond, E.C., 1957. Oceanographic studies in the Bay of Bengal. *Proceedings of the Indian Academy of Sciences* 46B, 1–46.
- Legendre, L., Rassoulzadegan, F., 1996. Food web mediated export of biogenic carbon in oceans: hydrodynamic control. *Marine Ecology Progress Series* 145, 179–193.
- Lukas, R., Lindstrom, E., 1991. The mixed layer of the western equatorial Pacific Ocean. *Journal of Geophysical Research* 96, 3343–3357.
- Madhu, N.V., Maheswaran, P.A., Jyothibabu, R., Sunil, V., Revichandran, C., Balasubramanian, T., Gopalakrishnan, T.C., Nair, K.K.C., 2002. Enhanced biological production off Chennai triggered by October 1999 super cyclone Orissa. *Current Science* 82, 1472–1479.

- Madhupratap, M., Nair, S.R., Haridas, P., Padmavathy, Gadi, 1990. Response of Zooplankton to physical changes in the environment: coastal upwelling along the Central West Coast of India. *Journal of Coastal Research* 62, 413–426.
- Madhupratap, M., Gauns, Mangesh, Ramaiah, N., Prasanna Kumar, S., Muraleedharan, P.M., De Sousa, S.N., Sardesai, S., Muraleedharan, Usha, 2003. Biogeochemistry of the Bay of Bengal: Physical, chemical and primary productivity characteristics of the central and western Bay of Bengal during summer monsoon 2001. *Deep-Sea Research II* 50, 881–896.
- Martin, A.P., Richards, K.J., 2001. Mechanisms for vertical nutrient transport within a North Atlantic mesoscale eddy. *Deep-Sea Research II* 48, 757–773.
- McGillicuddy, D.J., Robinson, A.R., 1997. Eddy induced nutrient supply and new production in the Sargasso Sea. *Deep-Sea Research I* 44, 1427–1450.
- Murty, C.S., Varadachari, V.V.R., 1968. Upwelling along the east coast of India. *Bulletin of National Institute of Sciences India* 361, 80–86.
- Nair, S.R., Vijayalekshmi, R. Nair., Achuthankutty, C.T., Madhupratap, M., 1981. Zooplankton composition and diversity in western Bay of Bengal. *Journal of Plankton Research* 34, 493–508.
- Pakhomov, E.A., Perissinotto, R., 1997. Mesozooplankton community structure and grazing impact in the region of the subtropical convergence south of Africa. *Journal of Plankton Research* 19, 675–691.
- Panikkar, N.K., Rao, T.S.S., 1973. Zooplankton investigation in the Indian waters and the role of the Indian Ocean Biological Centre. *Papers on the International Zooplankton Collections. IOBC Handbook. IOBC.* pp. 111–162.
- Pickett, M.H., Paduan, J.D., 2003. Ekman transport and pumping in the California Current based on the U.S. Navy's high-resolution atmospheric model COAMPS. *Journal of Geophysical Research* 108 (C10), 3327. doi:10.1029/2003JC00190.
- Prasad, T.G., 1997. Annual and seasonal mean buoyancy fluxes for the tropical Indian Ocean. *Current Science* 738, 667–674.
- Prasannakumar, S., Muraleedharan, P.M., Prasad, T.G., Gauns, M., Ramaiah, N., de Souza, S.N., Sardesai, S., Madhupratap, M., 2002. Why is the Bay of Bengal less productive during summer monsoon compared to the Arabian Sea? *Geophysical Research Letters* 29 (24), 2235. doi:10.1029/2002GL01601.
- Prasannakumar, S., Nuncio, M., Kumar, Ajoy, Narvekar, Jayu, Sardesai, S., Desouza, S.N., Gauns, M., Ramaiah, N., Madhupratap, M., 2004. Are eddies nature's trigger to enhance biological productivity in the Bay of Bengal? *Geophysical Research Letters* 31, L07309. doi:10.1029/2003GL01927.
- Qasim, S.Z., 1977. Biological productivity of the Indian Ocean. *Indian Journal of Marine Sciences* 6, 122–137.
- Rao, T.V.N., 2002. Spatial distribution of upwelling off the central east coast of India. *Estuarine and Coastal. Shelf Science* 542, 141–156.
- Rejomon, G., 2006. Biogeochemistry of trace metal in the Indian EEZ of the Arabian sea and Bay of Bengal. Ph. D Thesis, Cochin University of Science and Technology, India.
- Senguptha, R., De Sousa, S.N., Joseph, T., 1977. On nitrogen and phosphorous in the western Bay of Bengal. *Indian Journal of Marine Sciences* 6, 107–110.
- Shankar, D., Vinayachandran, P.N., Unnikrishnan, A.S., 2002. The monsoon currents in the north Indian Ocean. *Progress in Oceanography* 52, 63–70.
- Shetye, S.R., Sheno, S.S.C., Gouveia, A.D., Michael, G.S., Nampoothiri, D., Sundar, G., 1991. Wind-driven coastal upwelling along the western boundary of the Bay of Bengal during the southwest monsoon. *Continental Shelf Research* 11, 1397–1408.
- Shetye, S.R., Gouveia, A.D., Shankar, D., Sheno, S.S.C., Vinayachandran, P., Sundar, N., Michael, G.S., Namboodiri, G., 1996. Hydrography and circulation in the western Bay of Bengal during the northeast monsoon. *Journal of Geophysical Research* 101, 14011–14025.
- Sprintall, J., Tomczak, M., 1992. Evidence of barrier layer in the surface layer of the tropics. *Journal of Geophysical Research* 97, 7305–7316.
- Strickland, J.D.H., Parsons, T.R., 1972. A practical handbook of sea water analysis. *Bulletin of Fisheries Research Board Canada* 167, 310.
- Thunell, R.C., Reynolds, L.A., 1984. Sedimentation of Planktonic foraminifera: seasonal changes in species flux in the Panama Basin. *Micropaleontology* 30, 241–260.
- Udayavarma Thirupad, P., Gangadhara Reddy, C.V., 1959. Seasonal variations of the hydrological factors of the Madras coastal waters. *Indian Journal of Fisheries* 2, 298–302.
- UNESCO, 1988. River inputs into Ocean systems: status and recommendations for research. UNESCO Technical papers in marine science, No. 55, Final report of SCOR Working Group 46, Paris, 25pp.
- UNESCO, 1994. Protocols for the joint global ocean flux study. *Manual and Guides* 29, 190.
- Varkey, M.J., Murty, V.S.N., Suryanarayana, A., 1996. Physical oceanography of Bay of Bengal. *Oceanography and Marine Biology: An Annual Review*, vol. 34. University College London Press, London, pp. 1–70.
- Vinayachandran, P.N., Murty, V.S.N., Ramesh Babu, V., 2002. Observations of barrier layer formation in the Bay of Bengal during summer monsoon. *Journal of Geophysical Research* 107, C12. doi:10.1029/2001JC00083.